# Diagnostic efficacy of intravascular ultrasound combined with $Gd_2O_3$-EPL contrast agent for patients with atherosclerosis

SHUANGLI ZHU[1,2], CHAOYANG WEN[2], DONGXUE BAI[2] and MEIYING GAO[2]

[1]Department of Ultrasonic Medicine, Beijing Royal Integrative Medicine Hospital;
[2]Department of Ultrasonic Medicine, Peking University International Hospital, Beijing 102206, P.R. China

Received September 28, 2018; Accepted August 16, 2019

DOI: 10.3892/etm.2020.9265

**Abstract.** Atherosclerosis is a cardiovascular disease that is pathologically associated with the growth of atherosclerotic plaques and vascular vulnerability. Intravascular ultrasound (IVUS) has been used to evaluate and treat cardiovascular diseases. Accumulating evidence has demonstrated that $Gd_2O_3$-doped nanoparticles contrast can be applied for the diagnosis of human diseases. In the present study, eplerenone (EPL), a mineralocorticoid receptor antagonist, was first doped with $Gd_2O_3$ nanoparticles ($Gd_2O_3$-EPL), following which its diagnostic efficacy for use in IVUS measurements ($Gd_2O_3$-EPL-IVUS) was evaluated for patients suspected with atherosclerosis. $Gd_2O_3$-EPL-IVUS presented with higher accuracy and sensitivity compared with IVUS in diagnosing 188 patients with suspected atherosclerosis. $Gd_2O_3$-EPL-IVUS exhibited stronger signals associated with plaque morphology compared with aloe IVUS for patients with atherosclerosis. In addition, $Gd_2O_3$-EPL-IVUS application resulted in clearer arterial plaque images compared with IVUS by binding mineralocorticoid receptors. Atherosclerosis was subsequently confirmed in all patients using computerized tomography-coronary angiography. $Gd_2O_3$-EPL-IVUS showed more accuracy in measuring vessel size, plaque burden and minimal lumen area compared with IVUS analysis alone. In conclusion, these outcomes suggest that $Gd_2O_3$-EPL-IVUS is a reliable tool for the evaluation of coronary lesions in patients with atherosclerosis.

## Introduction

Atherosclerosis is a cardiovascular disease and a systemic chronic inflammatory disease that predominantly affects medium-sized arteries (1). Atherosclerosis is characterized by autoimmune response damage to the arterial wall accompanied with the subintimal accumulation of lipids, vascular smooth muscle cells and immunocompetent cells, which is pathologically associated with atherosclerotic plaque development and vascular vulnerability (2-4). In particular, pathology analysis revealed that the crucial event in the initiation and development of atherosclerosis is endothelial injury (5-7). Previous studies have suggested that atherosclerosis is a multifactorial disease triggered and sustained by a variety of risk factors including smoking, dyslipidemia, arterial hypertension and diabetes mellitus (4,8,9).

At present a number of techniques, including transesophageal echocardiography, epiaortic ultrasound, magnetic resonance imaging (MRI) and 3D ultrasound have been applied for diagnosis of atherosclerosis (10). A study has summarized current evidence regarding the role of intracoronary imaging for the diagnosis and risk stratification of coronary atherosclerosis (11). In addition, panoramic radiography offers a cost-effective approach in which early carotid artery calcification diagnosis and subsequent interventions can be performed (5). Ultrasound imaging have been widely applied for the diagnosis of atherosclerosis (12-15). Intravascular ultrasound (IVUS) is a more often used technique compared with thoracic ultrasound for the diagnosis of coronary artery disease, myocardial infarction and carotid atherosclerosis (16). Although IVUS has proven to be a highly valuable tool for the evaluation of mild-to-moderate coronary lesions (17), improvements in the diagnostic efficacy of IVUS imaging for patients with atherosclerosis is still required.

Contrast-enhanced ultrasound can be used for the diagnosis of different types of human atherosclerosis diseases, including coronary artery disease and peripheral artery disease (18). Of interest, nanoparticle technology such as $Gd_2O_3$ incorporate a variety of agents including anticancer compounds, fluorescent dyes and metal ions through physical encapsulation, covalent coupling or affinity binding for therapeutic or diagnostic applications (19). In particular, $Gd_2O_3$-albumin-conjugating photosensitizers can generate clearer signals *in vivo* during MRI diagnosis when coupled with enhanced imaging contrast for the effective localization of tumors (20). Additionally, $Gd_2O_3$ nanocrystal-based nanocomposites have been reported to serve as an ideal dual-mode contrast-enhancing agent for MRI by improving longitudinal reflexivity (21), which

*Correspondence to:* Professor Shuangli Zhu, Department of Ultrasonic Medicine, Beijing Royal Integrative Medicine Hospital, 1 Wangfu Street, Beijing 102206, P.R. China
E-mail: shuanglizhuprof@163.com

*Key words:* atherosclerosis, intravascular ultrasound, $Gd_2O_3$-doped mineralocorticoid receptor antagonism eplerenone nanoparticles contrast

may provide a versatile platform for molecular imaging and targeted drug delivery in ultrasound-facilitated diagnosis for human diseases (22).

Mineralocorticoid receptors are downstream effectors of angiotensin-II signaling in early atherosclerosis (23). A number of studies have recently found that mineralocorticoid receptor antagonists can regulate vascular function and/or contribute to vascular dysfunction (24-26). Eplerenone (EPL) is a specific mineralocorticoid receptor antagonist which has been shown to strengthen endothelium-dependent relaxation and suppress angiotensin-converting enzyme activity in the vasculature, thereby inhibiting the development of atherosclerosis (27).

In the present study, $Gd_2O_3$-coated EPL ($Gd_2O_3$-EPL) were used as the nanoparticles contrast to explore the diagnostic efficacy of $Gd_2O_3$-EPL combined with IVUS for patients with suspected atherosclerosis. This study also analyzed differences in the data obtained regarding vessel size, plaque burden and minimal lumen area using IVUS and $Gd_2O_3$-EPL-IVUS techniques.

## Materials and methods

*Participants*. A total of 188 patients (sex, 94 men and 94 women; mean age, 54±12 years; age range, 47-68) with suspected atherosclerosis were admitted to the Peking University International Hospital (Beijing, China) between April 2014 and May 2016 were recruited into the present study. The inclusion criteria are as follows: i) Age of individuals >25 years; ii) individuals exhibited hypertension, coronary heart disease and hyperlipidemia; and iii) individuals provided informed consent for participation. The exclusion criteria for all patients were as follows: i) Patients with history of cancer; ii) patients who underwent coronary artery surgery; and iii) patients who underwent heart stent surgery. Following recruitment, all included patients underwent IVUS followed by $Gd_2O_3$-EPL-IVUS 4 weeks later. CT coronary angiography was then performed at four-week intervals. The Ethical Committee of the Peking University International Hospital (approval no. LK20131018) approved this study. Written informed consent was provided by all patients.

*Contrast agent*. The $Gd_2O_3$-coated EPL contrast agents were synthesized as described previously (28). Briefly, cetyltrimethylammonium bromide ($C_{16}$TAB, 0.2 g) was first dissolved in distilled water (50 ml). $NH_3.H_2O$ (2 ml 25%) and tetraethoxysilane (4.49 mmol) were then added and the subsequent mixture was stirred at room temperature for 10 min. $Gd_2O_3$ (0.5 mmol) was added to this solution and stirred at 42˚C for 1 h before EPL (0.1 mmol) was added to the solution and stirred at room temperature for 1 h. Samples were calcined at 37˚C for 72 h before the $Gd_2O_3$-EPL nanoparticles were harvested. The purity and chemical structure of $Gd_2O_3$-EPL was determined by mass spectrometry as described previously (29). This resultant nanoparticle contrasting agent would be used for visualization for IVUS. All individuals received intravenously injections of $Gd_2O_3$-EPL contrast agents (0, 0.4, 0.8, 1.2, 1.6, 2.0, 2.4, 2.8, 3.2, 3.6 and 4.0 mg/kg) 2 h prior to IVUS. The application of $Gd_2O_3$-EPL contrast agents was approved by China Food and Drug Administration.

*Biochemical Analysis*. Blood samples (10 ml) were collected from each individual following overnight fasting for 12 h. Serum was obtained by centrifugation at 8,000 x g for 15 min at 4˚C. Total serum levels of triglyceride, cholesterol, low-density lipoprotein (LDL) cholesterol and high-density lipoprotein (HDL) cholesterol were measured using a TBA2000FR biochemical analyzer (Toshiba Corporation) as described previously (30). Metabolism of $Gd_2O_3$-EPL was then determined using inductively coupled plasma mass spectrometry (ICP-MS; Elan DRC II; PerkinElmer, Inc.) according to a previous study (31).

*Intravascular ultrasound virtual histology examination*. IVUS examination was performed as described previously (32). All patients received nonionic contrast medium $Gd_2O_3$-EPL (1.2 mg/ml). IVUS was subsequently performed using a 20 MHz catheter (2.9F monorail, 0.6 mm/s automatic pullback) after injection using a dedicated IVUS console (Volcano Corporation; Philips Healthcare) 2 h following intracoronary administration of 10 $\mu$g nitroglycerin. The IVUS images were captured at 30 frames/s using a DVD-Rom for subsequent offline analysis (Volcano Corporation; Philips Healthcare) and recorded into high-resolution super VHS videotapes. Signal intensity was determined from digital imaging and communications in medicine-stored images using a new Medical Imaging Bench system (version 4.0; Echoplaque-MIB; INDEC Medical systems, Inc.).

*Acquisition of carotid ultrasound index*. The carotid ultrasound index of individuals was analyzed using a Siemens ACUSON Sequoia™ Ultrasound system (Volcano Corporation; Philips Healthcare). The probe frequency was defined at 12 MHz. Ultrasound was performed to evaluate wall thickness in the carotid artery by an experienced professional sonographer. The mean intimal-medial thickness (IMT) was measured and the number of plaques in left anterior descending (LAD) artery in all individuals was counted. During the ultrasound measurement, the systolic lumen diameter ($D_s$), the diastolic lumen diameter ($D_d$), the systolic pressure ($P_s$), and diastolic pressure ($P_d$) of the carotid artery were input. The arterial compliance (AC) was measured using the following formula: $AC=\pi(D_s^2-D_d^2)/[4(P_s-P_d)]$ (33). The degree of plaque was graded using the $CHADS_2$ method on a scale from 0 to 3 (0, no observable plaque; 1, one small plaque <30% of lumen diameter; 2, one medium plaque 30-50% of vessel diameter; 3, one large plaque 50% of vessel diameter) as described previously (34). Plaque volume was calculated from the IVUS images as the total volume of the external elastic membrane occupied by the atheroma. Plaque burden was calculated as plaque and media cross-sectional area/external elastic membrane cross-sectional area. Plaque morphology was assessed on IVUS images of the LAD. Velocity vector imaging (VVI) was performed using the VVI software (syngo® US workplace; Siemens Healthineers) to evaluate speed of blood flow and data were analyzed by two independent pathologists.

*$CHADS_2$ scoring*. $CHADS_2$ scores were used to predict the degree of carotid atherosclerosis. The percentage of excess risk as calculated using the $CHADS_2$ scoring system was determined according to current guidelines as described previously (35).

Table I. Baseline clinical characteristics of patients with suspected atherosclerosis.

| Characteristics | Values |
|---|---|
| Male (n, %) | 94 (50%) |
| Female (n, %) | 94 (50%) |
| Age (years) | |
| Mean | 54±12 |
| Range | 47-68 |
| Hypertension (n, %) | 134 (71.3%) (>120 mmHg) |
| Body mass index (kg/m$^2$ ± SD) | 24.30±3.40 (healthy range, 18.5-24.0) |
| Cholesterol (mmol/l ± SD) | 4.88±0.76 (healthy range, 3.0-5.2) |
| HDL cholesterol (mmol/l ± SD) | 1.40±0.28 (healthy range, 1.0-2.0) |
| LDL cholesterol (mmol/l ± SD) | 2.85±0.80 (healthy range, 2.0-3.0) |
| Triglycerides (mmol/l ± SD) | 1.62±0.84 (healthy range, 3.5-4.0) |

HDL, high density lipoprotein; LDL, low density lipoprotein; SD, standard deviation.

*Coronary angiography*. CT-coronary angiography was performed using a dual-source CT scanner (SOMATOM Definition Flash; Siemens AG) according to standard techniques as described previously (36). All patients received 370 mg I/ml Ultravist® nonionic contrast medium (Schering AG) using a dual-head power injector (SCT-210; Medrad, Inc; Bayer AG). Measurements of vessel geometry, plaque burden and plaque morphology using coronary angiography images were performed according to a previous study (37). Coronary angiography images in LAD were analyzed using a quantitative coronary angiography program (version 2.0; Medis Medical Imaging Systems) by two independent investigators.

*Statistical analysis*. The pilot trial sample size of this study was determined using the following formula: $N=(\mu_\alpha+\mu_\beta)^2/12(1-c)(p'-0.5)^2$ ($\mu$, standard deviation; $\alpha$, I error probability; $\beta$, II error probability; p, error probability; c, ration of group) (38). Data are presented as mean ± SD and statistical analyses were performed using SPSS 19.0 software (IBM Corp.). A receiver operator characteristic (ROC) curve was used to analyze sensitivity and specificity determined by Youden's index. The area under the curve (AUC) and the P-values were obtained using the SPSS software. Relative risk was expressed as HR with 95% confidence intervals (95% CI) and global $\chi^2$-analyzes utilized logistic regression and likelihood ratios test. Student's t-test was used to compare two independent groups of data. P<0.05 was considered to indicate a statistically significant difference.

## Results

*Patients*. The clinical characteristics of the patients in the present study are summarized in Table I. There were no statistically significant differences in the baseline clinical parameters between male and female patients with suspected atherosclerosis. All patients exhibited symptoms of hypertension, coronary heart disease, and hyperlipidemia.

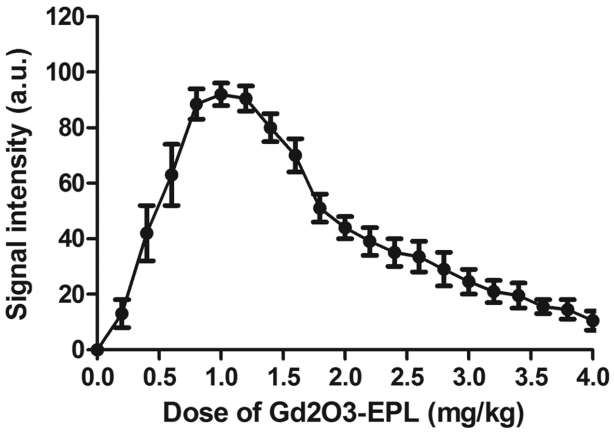


Figure 1. Determination of the optimal dose of $Gd_2O_3$-EPL in diagnosing carotid atherosclerosis based on signal intensity 2 h after injection. A range of doses of $Gd_2O_3$-EPL between 0 and 4.0 mg/kg was tested in patients with suspected atherosclerosis. EPL, eplerenone.

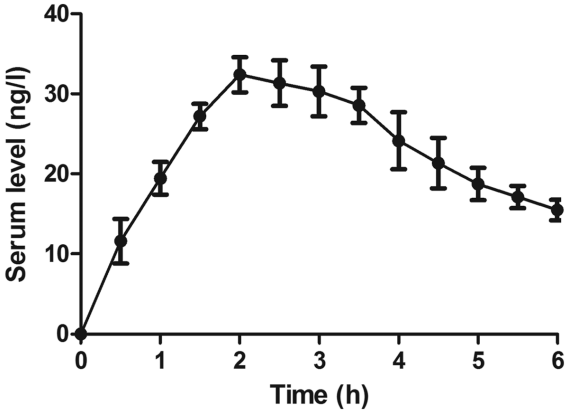


Figure 2. Determination of the optimal time for $Gd_2O_3$-EPL detection in diagnosing atherosclerosis after injection of 1.2 mg/kg of $Gd_2O_3$-EPL. Serum levels of $Gd_2O_3$-EPL in patients with suspected atherosclerosis was measured over a range of timepoints up to 6 h following injection with 1.2 mg/kg $Gd_2O_3$-EPL. EPL, eplerenone.

*Dose selection and detection time of $Gd_2O_3$-EPL*. Results identified 1.2 mg/kg $Gd_2O_3$-EPL to be the optimal dose in diagnosing carotid atherosclerosis based on signal intensity as measured using IVUS (Fig. 1). In addition, the maximal concentration of $Gd_2O_3$-EPL in the serum was attained 2 h following injection (Fig. 2). Therefore, 2 h post-injection was chosen as the timepoint for performing IVUS imaging on patients with suspected atherosclerosis.

*Diagnostic efficacy of $Gd_2O_3$-EPL-IVUS for patients with suspected atherosclerosis*. The present study explored the diagnostic efficacy of $Gd_2O_3$-EPL-IVUS in patients with suspected atherosclerosis. In total, $Gd_2O_3$-EPL-IVUS diagnosed 142 patients out of 188 patients with suspected atherosclerosis, whilst IVUS diagnosed 124 patients out of 188 patients with

Table II. Diagnostic efficacy of $Gd_2O_3$-EPL-IVUS for patients with suspected atherosclerosis.

| Patient | IVUS (n, %) | $Gd_2O_3$-EPL-IVUS (n, %) | P-value |
|---|---|---|---|
| Atherosclerosis | 124 (75.5) | 142 (66.0) | 0.048[a] |
| Non-atherosclerosis | 64 (24.5) | 46 (34.0) | 0.035[a] |

Statistical analysis was performed using Student's t-test. IVUS, intravascular ultrasound; EPL, eplerenone. [a]P<0.05 vs. IVUS.

Table III. Parameters diagnosed using $Gd_2O_3$-EPL-IVUS in patients with suspected atherosclerosis.

| Parameter | IVUS | $Gd_2O_3$-EPL-IVUS | P-value |
|---|---|---|---|
| IMT (mm) | 0.302±0.045 | 0.273±0.030 | 0.030[a] |
| $CHADS_2$ | 2.5±1.0 | 3.0±1.5 | 0.042[a] |
| AC ($mm^2$/kPa) | 2.00±0.82 | 3.50±0.96 | 0.016[a] |

[a]Statistical analysis was performed using Student's t-test. IMT, intimal-medial thickness; IVUS, intravascular ultrasound; EPL, eplerenone; AC, arterial compliance.

Table IV. Logistic regression of $Gd_2O_3$-EPL-IVUS to identify risk factors for atherosclerosis.

| Parameter | OR | 95% CI | P-value |
|---|---|---|---|
| Plaque index (r) | 1.062 | 0.078-0.096 | 0.024[a] |
| $CHADS_2$ score (r) | 0.462 | 1.042-1.684 | 0.020[a] |

[a]Statistical analysis was performed using $\chi^2$-test with logistic regression data. P-value was represented the statistical difference between $Gd_2O_3$-EPL-IVUS and IVUS. OR, odds ratio; CI, confidence interval; IVUS, intravascular ultrasound; EPL, eplerenone.

suspected atherosclerosis (Table II). ROC analysis also demonstrated that $Gd_2O_3$-EPL-IVUS exhibited higher accuracy and sensitivity compared with IVUS in diagnosing patients with suspected atherosclerosis (P<0.05; Fig. 3), since the AUC was 0.870 for the $Gd_2O_3$-EPL-IVUS group (95% CI, 0.858-0.882) and 0.782 for the IVUS group (95% CI, 0.772-0.792). These data suggest that $Gd_2O_3$-EPL-IVUS can accurately diagnose atherosclerosis by binding mineralocorticoid receptors in arterial lesions.

*Analysis of carotid ultrasound indices and VVI indices in patients diagnosed using IVUS and $Gd_2O_3$-EPL-IVUS.* Carotid Ultrasound Indices and VVI indices were subsequently compared between IVUS and $Gd_2O_3$-EPL-IVUS groups. The mean IMT was calculated to be 0.302±0.045 versus 0.273±0.030 diagnosed by IVUS and $Gd_2O_3$-EPL-IVUS, respectively. There were significant differences in the $CHADS_2$ scores between IVUS and $Gd_2O_3$-EPL-IVUS group (2.5±1.0 vs. 3.0±1.5, P<0.05). The arterial compliance (AC) index was 2.00±0.82 and 3.50±0.96 in patients diagnosed using IVUS and $Gd_2O_3$-EPL-IVUS, respectively (Table III).

*Comparison of atherosclerotic plaque characteristics using $Gd_2O_3$-EPL-IVUS or IVUS.* Multiple plaques were diagnosed on the same patient. The $Gd_2O_3$-EPL-IVUS technique observed stronger signals associated with the plaque morphology as determined by measuring signal intensity compared with IVUS in patients with atherosclerosis (Fig. 4). $Gd_2O_3$-EPL-IVUS resulted in clearer images of arterial plaques compared with IVUS (Fig. 5). $Gd_2O_3$-EPL-IVUS revealed arterial plaque lesions at higher frequencies compared with IVUS in the same patients with suspected atherosclerosis (Fig. 6).

*Logistic regression to identify risk factors for atherosclerosis.* According to the results of multivariate analysis, plaque index

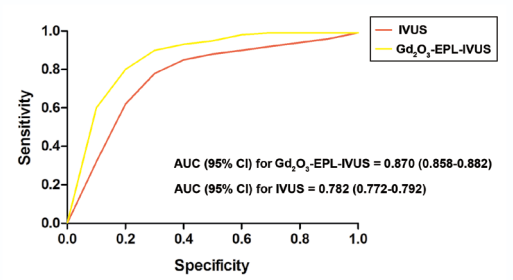


Figure 3. Receiver operating characteristic curve showing the accuracies and sensitivities of $Gd_2O_3$-EPL-IVUS and IVUS in diagnosing patients with suspected atherosclerosis. EPL, eplerenone; IVUS, intravascular ultrasound; AUC, area under the curve; CI, confidence interval.

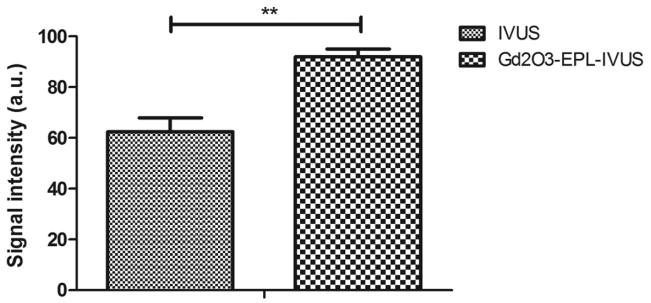


Figure 4. Signal intensity as derived from measurements of plaque burden and plaque volume in the coronary artery detected using $Gd_2O_3$-EPL-IVUS or IVUS in patients with atherosclerosis. **P<0.01. EPL, eplerenone; IVUS, intravascular ultrasound.

(OR, 1.062; 95% CI, 0.078-0.096) and $CHADS_2$ score (OR, 0.462; 95% CI, 1.042-1.684) was positively correlated with atherosclerosis diagnosis (Table IV). Taking either $CHADS_2$ scores or plaque index into consideration, $Gd_2O_3$-EPL-IVUS

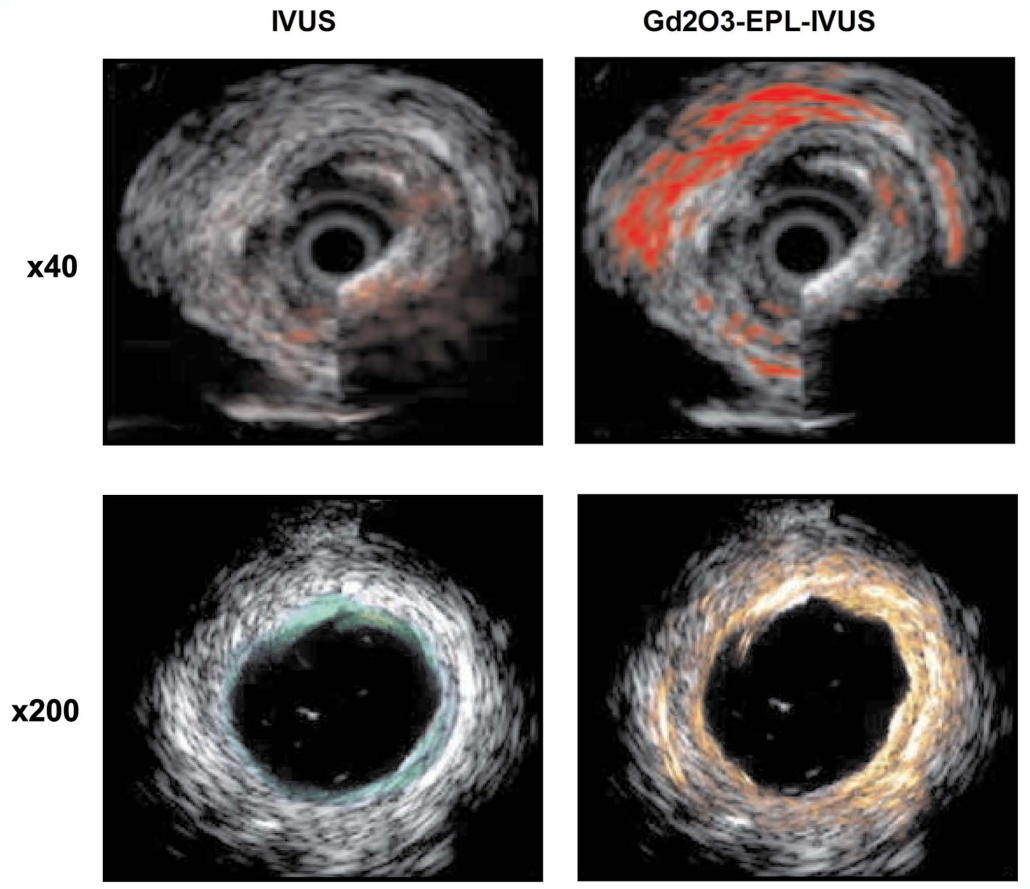


Figure 5. Images of atherosclerotic plaques taken using $Gd_2O_3$-EPL-IVUS or IVUS in the same patient with atherosclerosis. Magnification, x40 or x200. Color indicates the location of atherosclerosis inside the coronary artery. EPL, Eplerenone; IVUS, intravascular ultrasound.

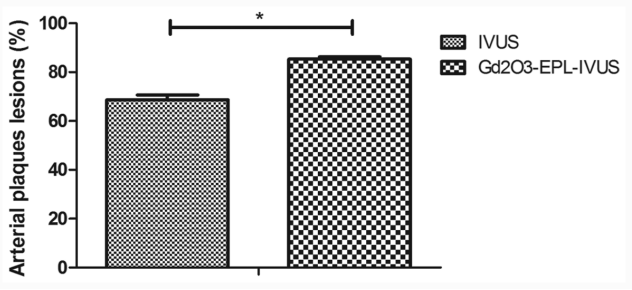


Figure 6. Comparison of frequencies of arterial plaque lesions in the coronary artery as diagnosed using $Gd_2O_3$-EPL-IVUS or IVUS in patients with suspected atherosclerosis. *P<0.05. EPL, esplerenone; IVUS, intravascular ultrasound.

was concluded to be a reliable method in predicting atherosclerotic lesions.

*Confirmation of atherosclerosis in patients using coronary angiography*. The atherosclerosis diagnosis in all patients as deduced using by $Gd_2O_3$-EPL-IVUS and IVUS were subsequently confirmed using coronary angiography. As shown in Fig. 7, representative coronary angiography images showed the presence of pathological atherosclerotic plaques in patients. Coronary angiography confirmed four false positive cases in 142/188 patients and three false negative cases in 46/188 patients following the use of $Gd_2O_3$-EPL-IVUS, whilst eight false positive cases in 124/188 and 29 false negative cases in 64/188 were reported as a result of IVUS (Table V).

*Pharmacodynamics of $Gd_2O_3$-EPL in plasma concentration in patients with atherosclerosis*. The serous metabolism of $Gd_2O_3$-EPL was investigated in patients with atherosclerosis. $Gd_2O_3$-EPL was fully metabolized within 12 h after injection (Fig. 8). No other side effects, including irritation on the injection site, hypertension and nausea, were observed in patients with atherosclerosis. These data suggest that $Gd_2O_3$-EPL is a safe contrast agent for use in IVUS in diagnosing patients with atherosclerosis.

## Discussion

Early and accurate diagnosis of atherosclerosis is crucial for the treatment of this disease (12,39,40). The present study is the first to examine the diagnostic efficacy of $Gd_2O_3$-EPL combined with IVUS for atherosclerosis in suspected patients, which provided evidence that $Gd_2O_3$-EPL-IVUS resulted in stronger signals associated with plaque morphology and generating clearer images of arterial plaques compared with IVUS alone. In addition, $Gd_2O_3$-EPL-IVUS uncovered higher frequencies of arterial plaque lesions and diagnosed atherosclerosis in patients with higher accuracy and sensitivity compared with IVUS alone.

Table V. Diagnostic efficacy of $Gd_2O_3$-EPL-IVUS for patients with suspected atherosclerosis.

| Type | IVUS (%) | $Gd_2O_3$-EPL-IVUS (%) | P-value |
|---|---|---|---|
| False positive (n, %) | 8 (6.5) | 4 (2.8) | 0.034[a] |
| True positive (n, %) | 116 (93.5) | 138 (97.2) | 0.049[a] |
| False negative (n, %) | 29 (45.3) | 3 (6.5) | <0.001[a] |
| True negative (n, %) | 35 (54.7) | 43 (93.5) | <0.001[a] |

[a]Statistical analysis was performed using $\chi^2$-test. IVUS, intravascular ultrasound; EPL, eplerenone.

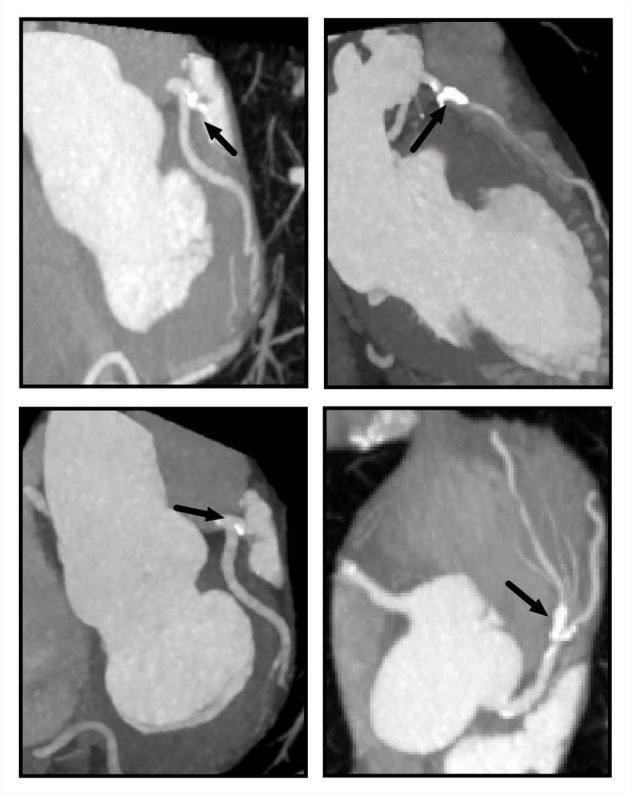

Figure 7. Confirmation of atherosclerosis diagnosis in different patients using computed tomography coronary angiography in the coronary artery. Arrows indicate the location of the atheromatous plaque. Magnification, x50.

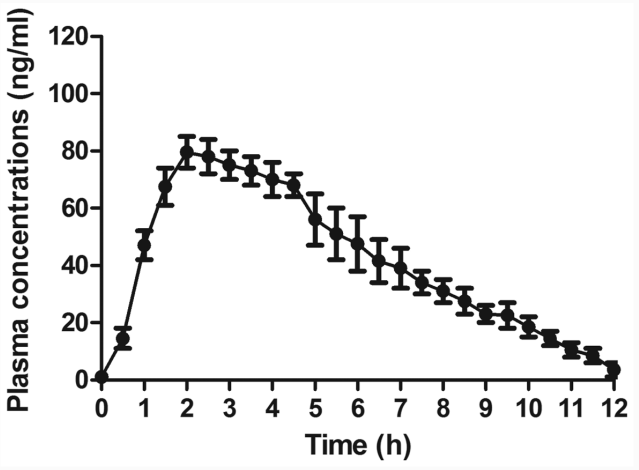


Figure 8. Plasma levels of $Gd_2O_3$-EPL in patients with suspected atherosclerosis over a time course of 12 h after injection of the contrast agent. EPL, Eplerenone; IVUS, intravascular ultrasound.

EPL is one of mineralocorticoid receptor antagonists where a previous study has found that EPL treatment reduced the sizes of lesions in early but not advanced atherosclerosis in Apolipoprotein E-deficient mice (41). EPL strengthened the endothelium-dependent relaxation and suppressed angiotensin-converting enzyme activity in the vasculature, which further prevented the development of atherosclerosis (24). Another study has previously found that IVUS can produce qualitative and quantitative images with high accuracies of plaque morphology identification in atherosclerosis lesions (5). In the present study, $Gd_2O_3$-EPL nanoparticles were introduced and it was found that the addition of $Gd_2O_3$-EPL enhanced the IVUS signals in evaluating the revascularization decision of intermediate and ambiguous coronary lesions. Previously, poor characterization of toxicity in the use of $Gd_2O_3$-$SiO_2$ core-shell nanoparticles was proving to be an obstacle to the clinical deployment for its application in diagnosis using MRI in xenografted murine tumors, due to its the accumulation in tissues (42). In the present study, $Gd_2O_3$-EPL and IVUS enhanced the diagnostic efficacy, independent of atherosclerosis severity. Specifically, data from the pharmacodynamics analysis in the present study suggest that $Gd_2O_3$-EPL may be a safe contrast agent for IVUS diagnosis due to its metabolism within 12 h after injection.

IVUS can be to predict and discriminate acute coronary syndrome culprit lesion phenotypes, which may help to diagnose active coronary plaques in preventing major adverse cardiac events in the future (43). In the present study, it was found that $Gd_2O_3$-EPL-IVUS enabled the accurate measurements of the vessel size, plaque burden and lumen area by binding with mineralocorticoid receptors. In addition, the application of $Gd_2O_3$-EPL also reduced the incidences of false positives and false negatives of IVUS in diagnosing patients suspected with atherosclerosis.

In conclusion, the findings in the present study suggest that $Gd_2O_3$-EPL-IVUS is a reliable tool for the evaluation of coronary lesions in patients with atherosclerosis. In addition, positive associations were found between the $CHADS_2$ scores and carotid ultrasound indicators and risk of atherosclerosis using data obtained from $Gd_2O_3$-EPL-IVUS in the present study, suggesting that images taken using $Gd_2O_3$-EPL-IVUS can reflect the degree of structural and functional impairment of atherosclerosis. Consequently, the application of $Gd_2O_3$-EPL-IVUS may contribute to the assessment of the

severity of atherosclerosis and the design of subsequent treatment strategies.

**Acknowledgements**

Not applicable.

**Funding**

No funding was received.

**Availability of data and materials**

The datasets used and/or analyzed during the current study are available from the corresponding author on reasonable request.

**Authors' contributions**

CYW and DXB made substantial contributions to the conception and prepared experiments. MYG was responsible for data acquisition, analysis and interpretation. SLZ designed this study, was involved in drafting the article and critically revising it for important intellectual content. All authors read and approved the final manuscript.

**Ethics approval and consent to participate**

The Ethical Committee of the Peking University International Hospital (approval no. LK20131018) approved this study. Written informed consent was provided by all patients.

**Patient consent for publication**

Not applicable.

**Competing interests**

The authors declare that they have no competing interests.

**References**

1. Yong WC, Sanguankeo A and Upala S: Association between sarcoidosis, pulse wave velocity, and other measures of subclinical atherosclerosis: A systematic review and meta-analysis. Clin Rheumatol 37: 2825-2832, 2018.
2. Zanoli L, Signorelli SS, Inserra G and Castellino P: Subclinical atherosclerosis in patients with inflammatory bowel diseases: A systematic review and meta-analysis. Angiology 68: 463, 2017.
3. Forgo B, Medda E, Hernyes A, Szalontai L, Tarnoki DL and Tarnoki AD: Carotid artery atherosclerosis: A review on heritability and genetics. Twin Res Hum Genet 21: 333-346, 2018.
4. Fava C and Montagnana M: Atherosclerosis is an inflammatory disease which lacks a common anti-inflammatory therapy: How human genetics can help to this issue. A narrative review. Front Pharmacol 9: 55, 2018.
5. Borba DL, Hipolito UV and Pereira YCL: Early diagnosis of atherosclerosis with panoramic radiographs: A review. J Vasc Bras 15: 302-307, 2016.
6. Moroni F, Ammirati E, Magnoni M, D'Ascenzo F, Anselmino M, Anzalone N, Rocca MA, Falini A, Filippi M and Camici PG: Carotid atherosclerosis, silent ischemic brain damage and brain atrophy: A systematic review and meta-analysis. Int J Cardiol 223: 681-687, 2016.
7. Anwaier G, Chen C, Cao Y and Qi R: A review of molecular imaging of atherosclerosis and the potential application of dendrimer in imaging of plaque. Int J Nanomedicine 12: 7681-7693, 2017.
8. Chen FH, Liu T, Xu L, Zhang L and Zhou XB: Association of serum vitamin D level and carotid atherosclerosis: A systematic review and meta-analysis. J Ultrasound Med 37: 1293-1303, 2018.
9. Mirnejad R, Razeghian-Jahromi I, Sepehrimanesh M, Zibaeenezhad MJ and Lopez-Jornet P: A proteomics analysis of the virulence factors of three common bacterial species involved in periodontitis and consequent possible atherosclerosis: A narrative review. Curr Protein Pept Sci 19: 1124-1130, 2018.
10. Jansen Klomp WW, Brandon Bravo Bruinsma GJ, van 't Hof AW, Grandjean JG and Nierich AP: Imaging techniques for diagnosis of thoracic aortic atherosclerosis. Int J Vasc Med 2016: 4726094, 2016.
11. Koskinas KC, Ughi GJ, Windecker S, Tearney GJ and Raber L: Intracoronary imaging of coronary atherosclerosis: Validation for diagnosis, prognosis and treatment. Eur Heart J 37: 524-535a-c, 2016.
12. Signorelli SS, Di Pino L, Fichera G, Celotta G, Pennisi G, Marchese G, Costa MP, Fallico R, Torrisi B and Virgilio V: Ultrasound diagnosis of carotid artery lesions in a population of asymptomatic subjects presenting atherosclerosis risk factors. J Stroke Cerebrovasc Dis 13: 95-98, 2004.
13. Mougiakakou SG, Golemati S, Gousias I, Nicolaides AN and Nikita KS: Computer-aided diagnosis of carotid atherosclerosis based on ultrasound image statistics, laws' texture and neural networks. Ultrasound Med Biol 33: 26-36, 2007.
14. Betriu-Bars A and Fernandez-Giraldez E: Carotid ultrasound for the early diagnosis of atherosclerosis in chronic kidney disease. Nefrologia 32: 7-11, 2012 (In Spanish).
15. Faust O, Acharya UR, Sudarshan VK, Tan RS, Yeong CH, Molinari F and Ng KH: Computer aided diagnosis of coronary artery disease, myocardial infarction and carotid atherosclerosis using ultrasound images: A review. Phys Med 33: 1-15, 2017.
16. Hibi K, Honda Y, Kimura K and Umemura S: Atherosclerosis: Progress in diagnosis and treatments. Topics: III. Progress in diagnosis of atherosclerosis; 5. IVUS (intravascular ultrasound). Nihon Naika Gakkai Zasshi 102: 344-353, 2013 (In Japanese).
17. Chen L, Xu T, Xue XJ, Zhang JJ, Ye F, Tian NL and Chen SL: Intravascular ultrasound-guided drug-eluting stent implantation is associated with improved clinical outcomes in patients with unstable angina and complex coronary artery true bifurcation lesions. Int J Cardiovasc Imaging 34: 1685-1696, 2018.
18. Jiang Y, Zhu J, Hu Y, Xing C, Li D and Hu B: Can scavenger receptor class B type I loaded ultrasound contrast agent be a new method for treating atherosclerosis? Med Hypotheses 73: 36-37, 2009.
19. Jeong H, Huh M, Lee SJ, Koo H, Kwon IC, Jeong SY and Kim K: Photosensitizer-conjugated human serum albumin nanoparticles for effective photodynamic therapy. Theranostics 1: 230-239, 2011.
20. Zhou L, Yang T, Wang J, Wang Q, Lv X, Ke H, Guo Z, Shen J, Wang Y, Xing C and Chen H: Size-Tunable $Gd_2O_3$@Albumin nanoparticles conjugating chlorin e6 for magnetic resonance imaging-guided photo-induced therapy. Theranostics 7: 764-774, 2017.
21. Wang FH, Bae K, Huang ZW and Xue JM: Two-photon graphene quantum dot modified $Gd_2O_3$ nanocomposites as a dual-mode MRI contrast agent and cell labelling agent. Nanoscale 10: 5642-5649, 2018.
22. Jung SH, Na K, Lee SA, Cho SH, Seong H and Shin BC: Gd(III)-DOTA-modified sonosensitive liposomes for ultrasound-triggered release and MR imaging. Nanoscale Res Lett 7: 462, 2012.
23. Keidar S, Hayek T, Kaplan M, Pavlotzky E, Hamoud S, Coleman R and Aviram M: Effect of eplerenone, a selective aldosterone blocker, on blood pressure, serum and macrophage oxidative stress, and atherosclerosis in apolipoprotein E-deficient mice. J Cardiovasc Pharmacol 41: 955-963, 2003.
24. Greenberg B: Mineralocorticoid receptor antagonists in heart failure: They work better when patients use them. Eur J Heart Fail 20: 1335-1337, 2018.
25. Shiota M, Fujimoto N, Higashijima K, Imada K, Kashiwagi E, Takeuchi A, Inokuchi J, Tatsugami K, Kajioka S, Uchiumi T and Eto M: Mineralocorticoid receptor signaling affects therapeutic effect of enzalutamide. Prostate: May 30, 2018 (Epub ahead of print).
26. Plieger T, Felten A, Splittgerber H, Duke E and Reuter M: Corrigendum to 'The role of genetic variation in the glucocorticoid receptor (NR3C1) and mineralocorticoid receptor (NR3C2) in the association between cortisol response and cognition under acute stress' [Psychoneuroendocrinology 87 (2018) 173-180]. Psychoneuroendocrinology 94: 169-170, 2018.
27. Takai S, Jin D, Muramatsu M, Kirimura K, Sakonjo H and Miyazaki M: Eplerenone inhibits atherosclerosis in nonhuman primates. Hypertension 46: 1135-1139, 2005.

28. Shao Y, Tian X, Hu W, Zhang Y, Liu H, He H, Shen Y, Xie F and Li L: The properties of Gd2O3-assembled silica nanocomposite targeted nanoprobes and their application in MRI. Biomaterials 33: 6438-6446, 2012.
29. Li X, Hu J, Yin D and Hu X: Solid-phase extraction coupled with ultra high performance liquid chromatography and electrospray tandem mass spectrometry for the highly sensitive determination of five iodinated X-ray contrast media in environmental water samples. J Sep Sci 38: 1998-2005, 2015.
30. Zhang GM, Bai SM, Ma XB and Goyal H: A novel method for estimating low-density lipoprotein (LDL) levels: Total cholesterol and non-high-density lipoprotein (HDL) can be used to predict abnormal LDL level in an apparently healthy population. Med Sci Monit 24: 1688-1692, 2018.
31. Moustakas M, Hanc A, Dobrikova A, Sperdouli I, Adamakis IS and Apostolova E: Spatial heterogeneity of cadmium effects on salvia sclarea leaves revealed by chlorophyll fluorescence imaging analysis and laser ablation inductively coupled plasma mass spectrometry. Materials (Basel) 12: 2953, 2019.
32. Calvert PA, Obaid DR, O'Sullivan M, Shapiro LM, McNab D, Densem CG, Schofield PM, Braganza D, Clarke SC, Ray KK, *et al*: Association between IVUS findings and adverse outcomes in patients with coronary artery disease: The VIVA (VH-IVUS in vulnerable atherosclerosis) study. JACC Cardiovasc Imaging 4: 894-901, 2011.
33. Zhang P, Guo R, Li Z, Xiao D, Ma L, Huang P and Wang C: Effect of smoking on common carotid artery wall elasticity evaluated by echo tracking technique. Ultrasound Med Biol 40: 643-649, 2014.
34. Falcão JL, Falcão BA, Gurudevan SV, Campos CM, Silva ER, Kalil-Filho R, Rochitte CE, Shiozaki AA, Coelho-Filho OR and Lemos PA: Comparison between MDCT and Grayscale IVUS in a quantitative analysis of coronary lumen in segments with or without atherosclerotic plaques. Arq Bras Cardiol 104: 315-323, 2015 (In English, Portuguese).
35. Lip GY, Nieuwlaat R, Pisters R, Lane DA and Crijns HJ: Refining clinical risk stratification for predicting stroke and thromboembolism in atrial fibrillation using a novel risk factor-based approach: The euro heart survey on atrial fibrillation. Chest 137: 263-272, 2010.
36. Xu L and Sun Z: Coronary CT angiography evaluation of calcified coronary plaques by measurement of left coronary bifurcation angle. Int J Cardiol 182: 229-231, 2015.
37. Zhou Y, Tian F, Wang J, Yang JJ, Zhang T, Jing J and Chen YD: Efficacy study of olmesartan medoxomil on coronary atherosclerosis progression and epicardial adipose tissue volume reduction in patients with coronary atherosclerosis detected by coronary computed tomography angiography: Study protocol for a randomized controlled trial. Trials 17: 10, 2016.
38. Yin D, Matsumura M, Rundback J, Yoho JA, Witzenbichler B, Stone GW, Mintz GS and Maehara A: Comparison of plaque morphology between peripheral and coronary artery disease (from the CLARITY and ADAPT-DES IVUS substudies). Coron Artery Dis 28: 369-375, 2017.
39. Adams A, Bojara W and Schunk K: Early diagnosis and treatment of coronary heart disease in symptomatic subjects with advanced vascular atherosclerosis of the carotid artery (type III and IV b findings using ultrasound). Cardiol Res 8: 7-12, 2017.
40. Fujiyoshi A, Jacobs DR Jr, Alonso A, Luchsinger JA, Rapp SR and Duprez DA: Validity of death certificate and hospital discharge ICD codes for dementia diagnosis: The multi-ethnic study of atherosclerosis. Alzheimer Dis Assoc Disord 31: 168-172, 2017.
41. Raz-Pasteur A, Gamliel-Lazarovich A, Coleman R and Keidar S: Eplerenone reduced lesion size in early but not advanced atherosclerosis in apolipoprotein E-deficient mice. J Cardiovasc Pharmacol 60: 508-512, 2012.
42. Tian X, Yang F, Yang C, Peng Y, Chen D, Zhu J, He F, Li L and Chen X: Toxicity evaluation of Gd2O3@SiO2 nanoparticles prepared by laser ablation in liquid as MRI contrast agents in vivo. Int J Nanomedicine 9: 4043-4053, 2014.
43. Murray SW, Stables RH, Garcia-Garcia HM, Grayson AD, Shaw MA, Perry RA, Serruys PW and Palmer ND: Construction and validation of a plaque discrimination score from the anatomical and histological differences in coronary atherosclerosis: The liverpool IVUS-V-HEART (Intra vascular ultrasound-virtual-histology evaluation of atherosclerosis requiring treatment) study. EuroIntervention 10: 815-823, 2014.